

GENERATION OF ELECTROMAGNETIC ION CYCLOTRON WAVE BY HOT INJECTION OF ION BEAM FOR RING DISTRIBUTION WITH A.C. ELECTRIC FIELD IN JOVIAN MAGNETOSPHERE

 Garima Yadav^a,  B.S. Sharma^a,  Ankita^{b*}

^aDepartment of Physics, Lords University, Alwar-301001, India

^bDepartment of Physics, Amity Institute of Applied Sciences, Amity University, Sector-125 Noida, Uttar Pradesh, India

*Corresponding Author e-mail: ankitac@amity.edu

Received September 11, 2024; revised November 29, 2024; in final form December 20, 2024; accepted January 7, 2025

This paper investigates the electromagnetic ion-cyclotron waves detected by the Ulysses spacecraft within the Jovian magnetosphere. Various types of high-frequency radio emissions resulting from resonant interactions have been identified in this region. The study focuses on the wave-particle interactions between electromagnetic ion-cyclotron waves and fully ionized magnetospheric plasma particles, considering the parallel propagation of these waves. This allows for a detailed evaluation of the dispersion relation with a ring distribution in the presence of a parallel alternating current (AC) electric field within a collisionless magnetosphere of Jupiter. Using a method of characteristics and a kinetic approach, we derive an expression for the relativistic growth rate. Additionally, we analyze injection events recorded by the Galileo spacecraft through its energetic particle detector (EPD) in the Jovian magnetosphere. Following the injection of a hot ion beam, we conduct a parametric analysis of various plasma parameters, such as temperature anisotropy, AC frequency, and relativistic factors, to examine their effects on the growth rate, which is illustrated through plotted graphs.

Keywords: *Electromagnetic ion-cyclotron waves; Ring distribution; Hot ion injection; Jovian magnetosphere*

PACS: 52.35Fp, 94.30Ch, 96.30Pj

1. INTRODUCTION

Electromagnetic ion cyclotron (EMIC) waves, typically left-hand polarized, are generated by the anisotropic temperature distribution of ions, particularly those in the energy range of 10–100 keV [1]. These waves are primarily formed near the magnetic equator of planetary magnetospheres and propagate along magnetic field lines toward higher latitudes [2], [3], [4]. Jupiter, the largest planet in our solar system, is a gas giant with a unique magnetosphere that plays a key role in the planet's dynamic environment. The magnetosphere is primarily shaped by Jupiter's rapid rotation and metallic hydrogen interior, with additional influence from its extensive moon system [4]. In Earth's magnetosphere, EMIC waves are categorized by the gyro frequencies of hydrogen, helium, and oxygen ions, with distinct emissions in the H-band, He-band, and O-band. Previous studies have shown that EMIC waves interact with energetic ions and relativistic electrons, playing a crucial role in the energization of cold ions and the loss of high-energy particles [5], [6], [7], [8]. Particles interacting with EMIC waves can be scattered into the loss cone, leading to precipitation into the upper atmosphere [9]. Observational studies have also shown that EMIC waves can contribute to the heating of He⁺ ions and electrons [10]. Recent studies have shown that electromagnetic ion cyclotron (EMIC) waves in Jupiter's magnetosphere are generated by anisotropic ions, particularly in regions where ion density and temperature anisotropy are high [11], [12], [13]. For instance, EMIC waves observed in the post-noon to dusk sector are attributed to the thermal anisotropy of strong ions in the current ring region. This suggests that the formation of EMIC waves is closely linked to the presence of ion rings and the cooling of plasma in specific regions of the magnetosphere [14], [15], [16].

The Jovian magnetosphere is an extremely dynamic environment, characterized by intense electromagnetic fields that significantly influence the motion and energy distributions of charged particles. One such phenomenon observed in this environment is the ring distribution, a specific arrangement of particle energies and pitch angles. Ring distributions are often associated with non-thermal electron populations that exhibit an anisotropic energy distribution, commonly seen in the presence of alternating current (A.C.) electric fields. These fields are thought to play a critical role in the acceleration and transport of electrons, facilitating the formation of the ring-like structures [17].

Recent studies have highlighted the significance of wave-particle interactions in the Jovian magnetosphere, which can drive the development of these ring distributions. For instance, the interaction of energetic electrons with electromagnetic waves, particularly those in the ion cyclotron frequency range, can contribute to the formation of these anisotropic distributions. In particular, research using data from the Juno spacecraft has provided insights into the electric field structures in Jupiter's magnetosphere, shedding light on the role of A.C. electric fields in driving such particle dynamics [18]. Understanding these distributions is crucial not only for Jupiter but also for interpreting similar phenomena in other planetary systems and their impact on magnetospheric dynamics.

In this paper, an attempt has been made to study the effect of hot injection on electromagnetic ion-cyclotron instability in Jovian magnetosphere similarly cold beam injection for whistler waves have been studied by [19], [20] at Saturn. Energy exchange processes and plasma injection play an important role in Jupiter's dynamics. Firstly, a detailed

derivation is done for dispersion relation having ring distribution in the presence of parallel AC electric field for ion-cyclotron electromagnetic wave. Also, an expression has been derived from the growth rate in terms of temperature anisotropy and electric field for EMIC waves in anisotropic plasma. Finally, we have calculated the growth rate for Jovian magnetospheric condition at $L = 17 R_J$ and results have been discussed. This approach will be helpful to understand the physics behind the various types of broadband emissions detected in Jovian magnetosphere and ionosphere.

2. DISPERSION RELATION AND GROWTH RATE

The dispersion relation outlines the conditions under which a wave propagates and provides a relation between the wave vector and frequency of the propagating wave on basis of wave particle interaction phenomenon and transfer energy from the particle to waves affect the growth rate of the wave [21]. The dispersion for electromagnetic ion-cyclotron in an infinite magnetosphere of Jupiter for a generalized loss cone type distribution function having anisotropic temperature has been studied. The injection of energetic hot ions (H^+) affects the growth rate significantly. To calculate the dispersion relation and growth rate for electromagnetic ion-cyclotron wave in plasma, some certain assumptions are made to the analysis. A spatially homogenous collision-less anisotropic plasma is assumed in the same z direction of ambient magnetic field B and external AC electric field $E = E_0 \sin vt \hat{e}_z$ to get dispersion relation and considered small inhomogeneity in the interaction zone. Kinetic theory and linearization of Vlasov Maxwell equations are used and after separation of equilibrium and non-equilibrium parts the higher order terms are neglected. Now the general dispersion relation for relativistic case with parallel AC electric field from [20] of equation (9) is written as:

$$\epsilon_{ij}(k, \omega) = 1 + \sum_s \frac{4e_s^2 \pi}{(\beta m_s)^2 \omega^2} \sum_n \sum_p J_p(\lambda_2) \int \frac{\|S_{ij}^*\| d^3 p}{\omega - \frac{k_{\parallel} p_{\parallel}}{\beta m_e} - \frac{k_{\parallel} \Gamma_z}{\beta v} + p v - \frac{n \omega_c}{\beta}} \quad (1)$$

Where

$$\|S_{ij}^*\| = \begin{vmatrix} p_{\perp} U^* \left(\frac{n}{\lambda_1}\right)^2 J_n^2 & i p_{\perp} U^* \left(\frac{n}{\lambda_1}\right) J_n J_{n'} & p_{\perp} W^* \left(\frac{n}{\lambda_1}\right) J_n^2 \\ i p_{\perp} U^* \left(\frac{n}{\lambda_1}\right) J_n J_{n'} & -p_{\perp} U^* (J_{n'})^2 & i p_{\perp} W^* J_n J_{n'} \\ p_{\parallel} U^* \left(\frac{n}{\lambda_1}\right) J_n^2 & i p_{\parallel} U^* J_n J_{n'} & p_{\parallel} W^* J_n^2 \end{vmatrix}$$

$$U^* = C - k_{\parallel} D \left(\frac{p}{\lambda_2} - 1\right) + F$$

$$W^* = D \left(\frac{k_{\perp} n m_e \omega_c}{k_{\perp} p_{\perp}}\right) \left(\frac{p}{\lambda_2} - 1\right) - B \left(\frac{n m_e \omega_c}{k_{\perp} p_{\perp}}\right) + (\beta m_e \omega) \frac{\partial f_o}{\partial p_{\parallel}}$$

$$B = (\beta m_e) \frac{\partial f_o}{\partial p_{\parallel}} \left(\frac{k_{\perp} p_{\perp}}{\beta m_e}\right)$$

$$C = \frac{(\beta m_e)^2}{p_{\perp}} \frac{\partial f_o}{\partial p_{\perp}} \left(\omega - \frac{k_{\parallel} p_{\parallel}}{\beta m_e}\right) \frac{p_{\perp}}{\beta m_e}$$

$$D = \frac{(\beta m_e)^2}{p_{\perp}} \frac{\partial f_o}{\partial p_{\perp}} \left(\frac{p_{\perp}}{\beta m_e}\right) \left(\frac{\Gamma_z}{\beta v}\right)$$

$$F = (\beta m_e) \frac{\partial f_o}{\partial p_{\parallel}} \left(\frac{k_{\parallel} p_{\perp}}{\beta m_e}\right)$$

The Bessel function arguments are defined as

$$J_n'(\lambda_1) = \frac{dJ_n(\lambda_1)}{d\lambda_1}$$

$$\lambda_1 = \frac{k_{\perp} v_{\perp}}{\omega_c m_e} \text{ and } \lambda_2 = \frac{k_{\parallel} \Gamma_z}{\beta v^2}$$

Where, β is the relativistic factor and defined as $= 1/\sqrt{1 - \frac{v^2}{c^2}}$. $\Gamma_z = \frac{e E_0}{m_e}$, $v =$ Angular frequency of A.C. electric field $m_e = \frac{m_s}{\beta}$ and $\omega_c = \frac{e B_0}{m_e}$ = cyclotron frequency of electron; p_{\perp} and p_{\parallel} denote momenta perpendicular and parallel to the magnetic field. For parallel propagation electromagnetic wave, $\epsilon_{11} \pm i \epsilon_{12} = N^2$ where $N^2 = \frac{k^2 c^2}{\omega^2}$.

The general dispersion relation for relativistic case with parallel AC electric field is written as:

$$\frac{k^2 c^2}{\omega^2} = 1 + \sum_s \frac{4e_s^2 \pi}{(\beta m_s)^2 \omega^2} \sum_p J_p(\lambda_2) \int \frac{d^3 p}{2} p_{\perp} \begin{bmatrix} (\beta m_s) \left(\omega - \frac{k_{\parallel} p_{\parallel}}{\beta m_s} \right) \frac{\partial f_o}{\partial p_{\perp}} \\ -k_{\parallel} (\beta m_s) \frac{\partial f_o}{\partial p_{\perp}} \frac{\Gamma_z}{\beta v} \left(\frac{p}{\lambda_2} - 1 \right) \\ +k_{\parallel} p_{\perp} \frac{\partial f_o}{\partial p_{\parallel}} \end{bmatrix} * \left(\frac{1}{\omega - \frac{k_{\parallel} p_{\parallel}}{\beta m_s} - \frac{k_{\parallel} \Gamma_z}{\beta v} + p v \pm \frac{\omega_c}{\beta}} \right), \quad (2)$$

where, subscript ‘s’ denotes type of species i.e. electrons and ions.

The ring distribution function is assumed to be distribution function of the trapped particles from [10], [20], [22],

$$f(p_{\perp}, p_{\parallel}) = \frac{n_s/n}{\pi^{3/2} p_{o\parallel s} p_{o\perp s}^2 A} \exp \left[-\frac{(p_{\perp} - v_o)^2}{p_{o\perp s}^2} - \frac{(p_{\parallel}^2)}{p_{o\parallel s}^2} \right], \quad (3)$$

$$A = \exp \left(-\frac{v_o^2}{p_{o\perp s}^2} \right) + \sqrt{\pi} \left(\frac{v_o}{p_{o\perp s}} \right) \operatorname{erfc} \left(-\frac{v_o}{p_{o\perp s}} \right), \quad (4)$$

$p_{o\parallel e} = (k_b T_{\parallel e} / \beta m_e)^{1/2}$, $p_{o\perp e} = (k_b T_{\perp} / \beta m_e)^{1/2}$, $p_{o\parallel i} = (k_b T_{\parallel i} / \beta m_i)^{1/2}$ and $p_{o\perp i} = (k_b T_{\perp i} / \beta m_i)^{1/2}$ are the associated parallel and perpendicular thermal momenta of ions and electrons.

n_s/n in equation (3) represents the ratio of particle total density captured and characterized by high energy, and $\operatorname{erfc}(x)$ in equation (4) is a complementary error function. The drift velocity is represented as v_o .

Substituting $d^3 p = 2\pi \int_0^{\infty} p_{\perp} dp_{\perp} \int_{-\infty}^{\infty} dp_{\parallel}$ and using expression (2) in equation (1) and after solving the integrations, we get the dispersion relation as:

$$\frac{k^2 c^2}{\omega^2} = 1 + \frac{4e_s^2 \pi}{(\beta m_s)^2 \omega^2} \sum_p J_p(\lambda_2) \frac{(n_s/n)}{A} (\beta m_s) \left[\frac{\beta m_s}{p_{o\parallel s}} \left(\frac{\omega}{k_{\parallel}} - \frac{\Gamma_{\parallel s}}{\beta v} \left(\frac{p}{\lambda_2} - 1 \right) \right) X_1 Z(\xi) + X_2 (1 + \xi Z(\xi)) \right]. \quad (5)$$

The above dispersion relation is now approximated in ion cyclotron range of frequencies. In this case electrons temperature $T_{\perp e} = T_{\parallel e} = T_e$ are assumed and magnetized with $|\omega_r + i\gamma| \ll \omega_{ci}$ whereas ions are assumed to have the condition $T_{\perp i} > T_{\parallel i}$ and $|k_{\parallel} \alpha_{\parallel i}| \ll |\omega_r \pm \omega_{ci} + i\gamma|$, $\frac{\omega_{pe}^2}{\pm \omega_{ce}^2} = \frac{-\omega_{pi}^2}{\pm \omega_{ci}^2}$. So, considering these approximations, equation (5) becomes:

$$D(k, \omega_r + i\gamma) = 1 - \frac{k^2 c^2}{(\omega_r + i\gamma)^2} + \sum_p J_p(\lambda_2) \left[\left(\frac{\omega_{pe}^2}{\omega_{ci}^2} - \frac{\omega_{pe}^2}{(\omega_r + i\gamma)(\pm \omega_{ci})} \right) X_{1e}(\beta m_e) + \frac{\omega_{pi}^2}{(\omega_r + i\gamma)^2} \left(X_{1i} \frac{(\beta m_i)}{p_{o\parallel i}} \left(\frac{\omega_r + i\gamma}{k_{\parallel}} - \frac{\Gamma_{\parallel i}}{\beta v} \left(\frac{p}{\lambda_2} - 1 \right) \right) Z(\xi_i) + X_{2i} (1 + \xi_i Z(\xi_i)) \right) \right]. \quad (6)$$

Where,

$$X_{1i} = 1 + \frac{v_o^2}{p_{o\perp i}^2} - \sqrt{\pi} \frac{v_o}{p_{o\perp i}},$$

$$X_{1e} = 1 + \frac{v_o^2}{p_{o\perp e}^2} - \sqrt{\pi} \frac{v_o}{p_{o\perp e}} \text{ and}$$

$$X_{2i} = X_{1i} + \frac{p_{oLi}^2}{p_{oLi}^2} \left(1 - \sqrt{\pi} \frac{v_o^3}{p_{oLi}^3} \operatorname{erfc} \left(\frac{v_{Li}}{p_{oLi}} \right) + 3 \frac{v_o^2}{p_{oLi}^2} - \frac{3}{2} \sqrt{\pi} \frac{v_o}{p_{oLi}} \right)$$

After applying the condition $\left| \frac{k^2 c^2}{\omega^2} \gg 1 + \frac{\omega_{pe}^2}{\omega_{ce}^2} \right|$, the dispersion relation of above equation becomes

$$D(k, \omega_r + i\gamma) = -\frac{k_{\parallel}^2 c^2}{\omega_{pi}^2} + \sum_p J_p(\lambda_2) \left[\begin{array}{l} \frac{\omega}{\pm \omega_{ci}} (\beta m_e) X_{1e} \\ + (\beta m_i) X_{1i} \left\{ \frac{\beta m_i}{p_{oLi}} \left(\frac{\omega}{k_{\parallel}} - \frac{\Gamma_{\parallel i}}{\beta v} \left(\frac{p}{\lambda_2} - 1 \right) \right) Z(\xi_i) + \frac{X_{2i}}{X_{1i}} (1 + \xi_i Z(\xi_i)) \right\} \end{array} \right]. \quad (7)$$

The function of plasma dispersion is given by

$$Z(\xi) = \frac{1}{\sqrt{\pi}} \int_{-\infty}^{\infty} \frac{e^{-t^2}}{t - \xi} dt,$$

Where

$$\xi = \frac{\beta m_i \omega - k_{\parallel} \Gamma_{\parallel i} m_i / v + (\beta m_i) p v \pm m_i \omega_c}{k_{\parallel} p_{oLi}}; \quad \omega_{pi}^2 = \frac{4\pi e^2 n_i / n}{(\beta m_i)^2 B}$$

Now, dimensionless parameter wave vector $\tilde{k} = \frac{k_{\parallel} p_{oLi}}{\omega_{ci}}$ is introduced.

In case of Parallel propagation

The expression of growth rate and real frequency for the waves propagating parallel to magnetic field direction becomes:

$$\frac{\gamma}{\omega_{ci}} = \frac{\frac{\sqrt{\pi}}{\tilde{k}} \left(\frac{X_{2i}}{X_{1i}} - k_4 \right) k_3^3 \exp \left[-\left(\frac{k_3}{\tilde{k}} \right)^2 \right]}{1 + \frac{\tilde{k}^2}{2k_3^2} + \frac{\tilde{k}^2}{k_3} \left(\frac{X_{2i}}{X_{1i}} - k_4 \right) + \frac{m_e}{m_i} \frac{X_{1e}}{X_{1i}} k_3^2}. \quad (8)$$

The real part of eq. (8) is

$$X_3 = -\frac{\beta \omega_r}{\omega_c} = X_4 + \frac{\tilde{k}^2}{2\beta_1} \left[\frac{X_{2i}}{X_{1i}} \frac{\beta_1}{(1 + X_4)} - \frac{(1 + X_4)}{\beta X_{1i}} \right]$$

Where

$$k_3 = 1 - \beta X_3 + \beta X_4, \quad k_4 = \frac{\beta X_3 - \beta X_4}{1 - \beta X_3 + \beta X_4} \quad \text{and} \quad \beta_1 = \frac{4\pi \mu_0 \epsilon_0 k_b T_{\parallel i} (n_i / n)}{AB_0^2}; \quad X_4 = \frac{k_{\parallel} \Gamma_{\parallel i}}{\beta v \omega_c} - \frac{p v}{\omega_c}.$$

Magnetic field model used is taken from [23], [24], [25]

$$B = B_0 \left(\frac{[1 + 3 \sin^2 \theta]^{\frac{1}{2}}}{\cos^6 \theta} \right),$$

where

B_0 is magnetic field at equator and θ represents the magnetic latitude.

3. PLASMA PARAMETERS

Mauk et al [26] have reported injection events observed by Galileo spacecraft in Jupiter's magnetosphere at the radial distance between 9 and 27 R_J have reported in the energy range above 20 KeV. For the evaluation of growth rate inside Jupiter's magnetosphere to analyze the hot injection effect on electromagnetic ion-cyclotron wave with parallel propagation in Jovian magnetosphere at the radial distance $R \sim 17 R_J$ with $B_0 = 51$ nT [23] the set of background plasma

parameters are considered as number density of cold ions, $n_c = 3 \times 10^6 \text{ m}^{-3}$, temperature anisotropy, $A_T=2$, thermal energy of ions and electrons $K_B T_{||i} = 1 \text{ keV}$ and $K_B T_{||e} = 200 \text{ eV}$, and after injecting warm plasma, parameters are considered as number density of warm ions, $n_w = 3 \times 10^7 \text{ m}^{-3}$, temperature anisotropy, $A_T=1.75, 2, 2.25$, thermal energy of ions and electrons $K_B T_{||i} = 3 \text{ keV}$ and $K_B T_{||e} = 200 \text{ eV}$. Where, number density ratio of cold and warm ions, $n_c/n_w=1/10$. According to the previous study, Clark et al. [27] have reported that the approximate magnitudes of electric field and magnetic field are taken to be 10 mV/m and 51 nT respectively.

4. RESULT AND DISCUSSION

To study the variation of various plasma parameters on growth rate with the effect of hot injection for ring distribution function in the presence of AC electric field, mathematical calculations have been performed.

Figure 1 shows the variation of growth rate (γ/ω_c) with the effect of hot injection on ion-cyclotron wave with respect to increasing \tilde{k} for various values of AC frequency. Ring distribution function is assumed with the beam of energetic particles. Behavior of ion-cyclotron wave is shown in the graph by interaction of wave with hot injected particles in Jovian magnetosphere. AC frequency range has been taken from 2 Hz to 2.2 Hz. The growth rate (γ/ω_c) for $\nu = 2 \text{ Hz}$ is 4.84211×10^{-06} at $\tilde{k} = 0.35$, the growth rate (γ/ω_c) for $\nu = 2.1 \text{ Hz}$ is 0.000011353024571591 at $\tilde{k} = 0.35$ and for $\nu = 2.2 \text{ Hz}$, the growth rate is $\gamma/\omega_c = 0.000025023536544779$ at $\tilde{k} = 0.35$. It is clearly seen that growth rate increases as the values of AC frequency increases.

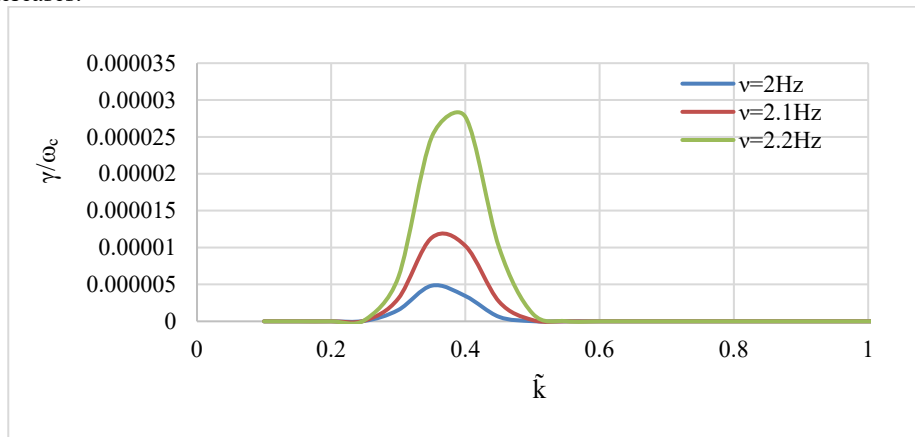


Figure 1. Variation of Growth Rate versus for different values of A.C. frequency at $B_0=5.1 \times 10^{-8} \text{ T}$, $A_T=1.5$, $K_B T_{||i}=1 \text{ keV}$, $K_B T_{||e}=200 \text{ eV}$, $E_0=0.1 \text{ V/m}$ and other fixed parameters of plasma at 17 R_J

In Figure 2, the variation of growth rate (γ/ω_c) with respect to increasing \tilde{k} with the hot injection effect on EMIC for various values temperature anisotropy of cold ions has been plotted. For $A_T = 1.5, 2$ and 2.5 , the peak values are observed at $\tilde{k} = 0.35, 0.35, 0.35$ and the growth rates are $\gamma/\omega_c = 3.41842223973875 \times 10^{-06}$, 0.0000169021159039714 and 0.0000720765136280518 respectively. Thus, the relativistic growth rate increases as temperature anisotropy of cold plasma increases. Usually the temperature anisotropy of ions is greater than the electron’s temperature anisotropy. Hence this condition leads to the wave growth reported by [28].

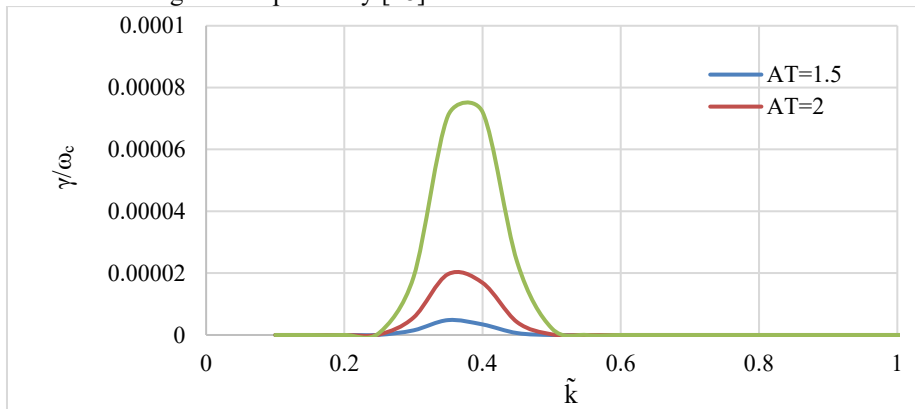


Figure 2. Variation of Growth Rate versus for different values of temperature anisotropy at $\nu=2 \text{ Hz}$, $K_B T_{||i}=1 \text{ keV}$, $K_B T_{||e}=200 \text{ eV}$, $B_0=5.1 \times 10^{-8} \text{ T}$, $E_0=0.1 \text{ V/m}$ and other fixed parameters of plasma at 17 R_J

Using Figure 3, variation of dimensionless growth rate in background plasma on EMIC wave in Jovian magnetosphere with respect to wave number \tilde{k} for different values of number density n_0 at other fixed parameters is shown. For $n_0=4 \times 10^6$,

the peak value of growth rate is $\gamma/\omega_c = 0.00023367$ appears at $\tilde{k} = 0.4$, for $n_0 = 5 \times 10^6$, growth rate is $\gamma/\omega_c = 0.002254457$ at $\tilde{k} = 0.45$ and as number density is increasing to $n_0 = 6 \times 10^6$, peak value $\gamma/\omega_c = 0.009471069$ at $\tilde{k} = 0.5$. So, as we increase number density n_0 from 4×10^6 to 6×10^6 , growth rate increases, and peaks appear at same wave number \tilde{k} .

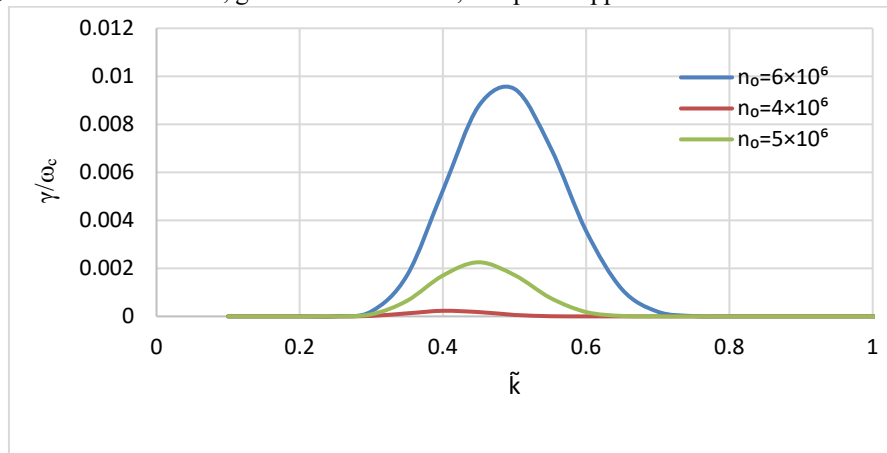


Figure 3. Variation of Growth Rate versus for different values of number density, n_0 at $\nu = 2$ Hz, $K_B T_{\parallel i} = 1$ keV, $K_B T_{\parallel e} = 200$ eV, $B_0 = 5.1 \times 10^{-8}$ T, $E_0 = 0.1$ V/m and other fixed parameters of plasma at $17 R_J$

Figure 4 shows the variation of growth rate (γ/ω_c) with the effect of background on ion-cyclotron wave with respect to increasing \tilde{k} for various values of AC frequency with effect of magnetic field model. Ring distribution function is assumed with the beam of energetic particles. Behavior of ion-cyclotron wave is shown in the graph by interaction of wave with hot injected particles in Jovian magnetosphere. AC frequency range has been taken from 2 Hz to 2.2 Hz. The growth rate (γ/ω_c) for $\nu = 2$ Hz is 6.3028×10^{-9} at $\tilde{k} = 0.35$, the growth rate (γ/ω_c) for $\nu = 2.1$ Hz is 2.2927×10^{-8} at $\tilde{k} = 0.35$ and for $\nu = 2.2$ Hz, the growth rate is $\gamma/\omega_c = 7.49878 \times 10^{-8}$ at $\tilde{k} = 0.35$. It is clearly seen that growth rate increases as the values of AC frequency increases.

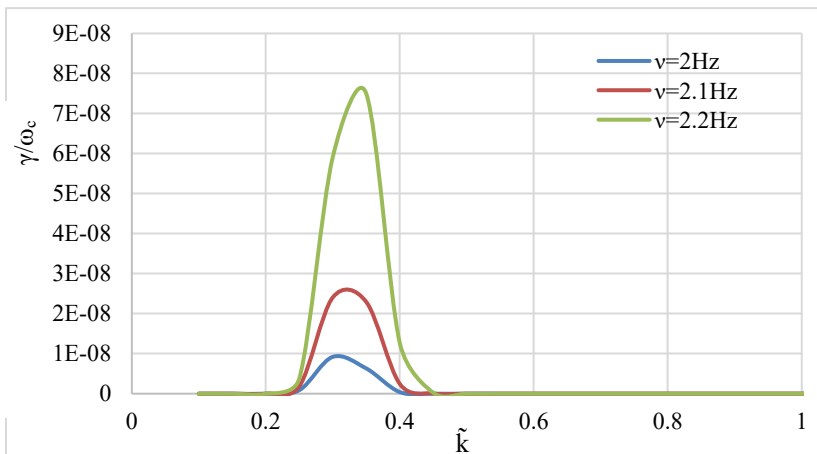


Figure 4. Variation of Growth Rate versus for different values of A.C frequency using magnetic field model at $B_0 = 5.1 \times 10^{-8}$ T, $A_T = 1.5$, $K_B T_{\parallel i} = 1$ keV, $K_B T_{\parallel e} = 200$ eV, $E_0 = 0.1$ V/m and other fixed parameters of plasma at $17 R_J$

In Figure 5, shows the effect of temperature anisotropy on growth rate with the effect of hot injected plasma with effect of magnetic field with respect to \tilde{k} of electromagnetic ion-cyclotron waves using ring distribution function in the Jovian magnetosphere. It can be seen that for $A_T = 1.5$ the maxima occurs at $\tilde{k} = 0.3$ with $\gamma/\omega_c = 9.1863 \times 10^{-9}$, for $A_T = 2$ the highest peak $\gamma/\omega_c = 4.24628 \times 10^{-8}$ occurs at $\tilde{k} = 0.3$ and for $A_T = 2.5$ the peak value $\gamma/\omega_c = 1.77683 \times 10^{-7}$ appears at $\tilde{k} = 0.3$. It shows that growth increases for parallel propagation of EMIC wave in Jupiter’s magnetosphere with increasing the magnitude of temperature anisotropy.

Figure 6 shows the effect of temperature anisotropy on growth rate with the effect of hot injected plasma with respect to \tilde{k} of electromagnetic ion-cyclotron waves using ring distribution function in the Jovian magnetosphere. It can be seen that for $A_T = 1.5$ the maxima occurs at $\tilde{k} = 0.55$ with $\gamma/\omega_c = 0.525446451$, for $A_T = 2$ the highest peak $\gamma/\omega_c = 0.589756008$ occurs at $\tilde{k} = 0.50$ and for $A_T = 2.5$ the peak value $\gamma/\omega_c = 0.658963625$ appears at $\tilde{k} = 0.5$. It shows that growth increases for parallel propagation of EMIC wave in Jupiter’s magnetosphere with increasing the magnitude of temperature anisotropy.

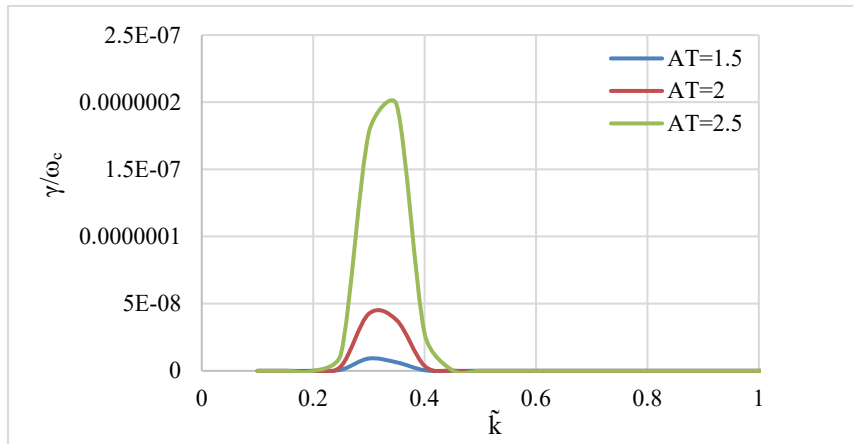


Figure 5. Variation of Growth Rate versus for different values of temperature anisotropy with magnetic field model at $\nu = 2$ Hz, $K_B T_{||i} = 1$ keV, $K_B T_{||e} = 200$ eV, $B_0 = 5.1 \times 10^{-8}$ T, $E_0 = 0.1$ V/m and other fixed parameters of plasma at 17 R_J

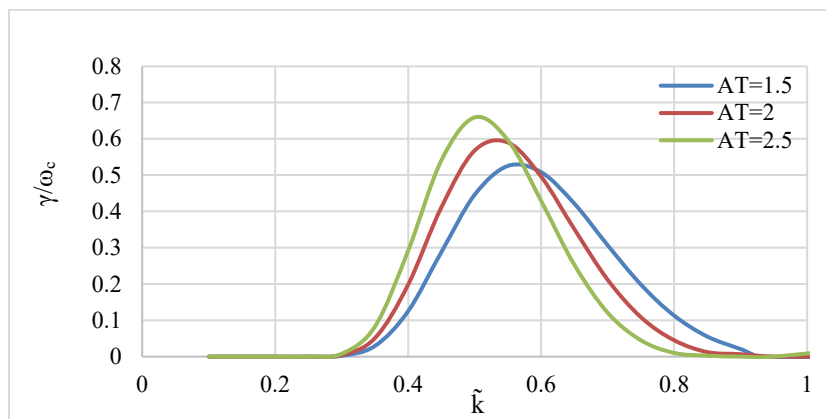


Figure 6. Variation of Growth Rate versus for different values of Temperature Anisotropy with beam at $n_c/n_w = 1/10$, $B_0 = 5.1 \times 10^{-8}$ T, $K_B T_{||i} = 1$ keV, $K_B T_{||ib} = 3$ keV, $K_B T_{||e} = 200$ eV and other fixed parameters of plasma at 17 R_J

Figure 7 shows the effect of relativistic factor on growth rate with the effect of hot injected plasma with respect to \tilde{k} of electromagnetic ion-cyclotron waves using ring distribution function in the Jovian magnetosphere. It can be seen that for $\beta = 0.7$ the maxima occurs at $\tilde{k} = 0.55$ with $\gamma/\omega_c = 0.525446451$, for $\beta = 0.8$ the highest peak $\gamma/\omega_c = 0.531257736$ occurs at $\tilde{k} = 0.50$ and for $\beta = 0.9$ the peak value $\gamma/\omega_c = 0.520711317$ appears at $\tilde{k} = 0.45$. It shows that growth rate shifts for higher value of wave number with decrease in the value of relativistic factor for parallel propagation of EMIC wave in Jupiter’s magnetosphere with increasing the magnitude of relativistic factor.

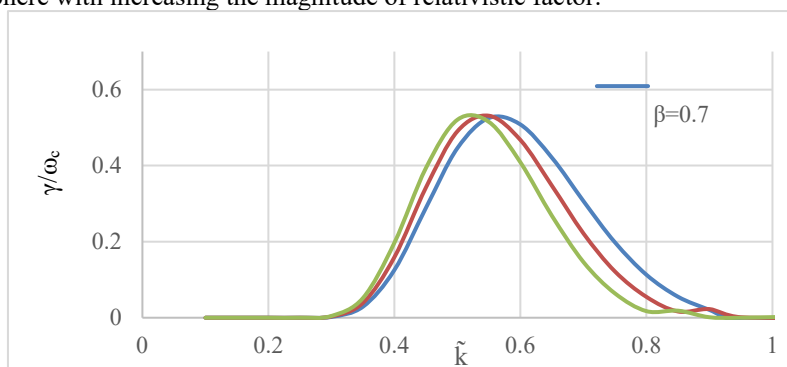


Figure 7. Variation of Growth Rate versus for different values of relativistic factor with beam at $n_c/n_w = 1/10$, $B_0 = 5.1 \times 10^{-8}$ T, $A_T = 1.5$, $K_B T_{||i} = 1$ keV, $K_B T_{||ib} = 3$ keV, $K_B T_{||e} = 200$ eV and other fixed parameters of plasma at 17 R_J

Figure 8 shows the effect of number density ratio of electrons and ions on growth rate after injecting hot plasma with respect to \tilde{k} of EMIC waves using ring distribution function at Jupiter. It can be observe that for $n_c/n_w = 1/10$ the maxima occurs at $\tilde{k} = 0.55$ with $\gamma/\omega_c = 0.525446451$, for $n_c/n_w = 1/20$ the highest peak $\gamma/\omega_c = 0.529429323$ occurs at $\tilde{k} = 0.55$ and for $n_c/n_w = 1/30$ the peak value $\gamma/\omega_c = 0.530342417$ appears at $\tilde{k} = 0.55$. It can be concluded that growth increases for parallel propagation of EMIC wave in Jupiter’s magnetosphere as the magnitude increases. Thus, number

density of electron does not affect the growth rate in the case of hot injection ion beam as [29], [30] that dependence of dispersive properties of EMIC wave are on density and thermal plasma composition of ions.

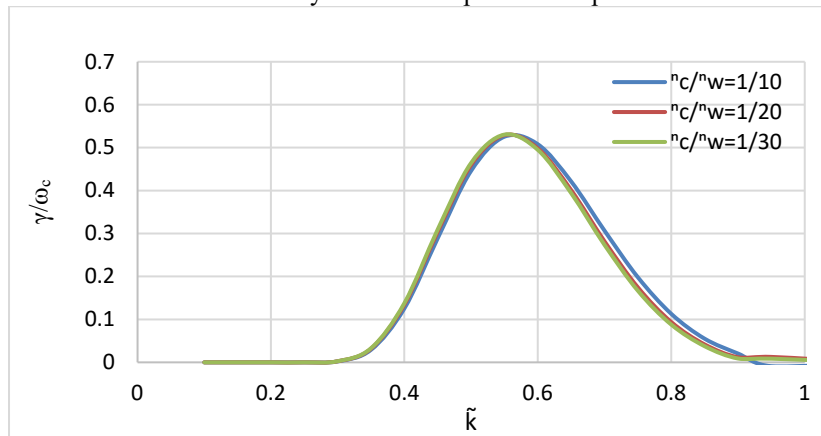


Figure 8. Variation of Growth Rate versus for different values of number density, n_0 , for $\nu = 2$ Hz, $K_B T_{||i} = 1$ keV, $K_B T_{||ib} = 3$ keV, $K_B T_{||e} = 200$ eV, $B_0 = 5.1 \times 10^{-8}$ T, $E_0 = 0.1$ V/m and other fixed parameters of plasma at $17 R_J$

Using Figure 9, variation of dimensionless growth rate in background plasma with the effect of hot injection on EMIC wave with magnetic field model in Jovian magnetosphere with respect to wave number \tilde{k} for different values of temperature anisotropy at other fixed parameters is shown. For $A_T = 1.75$, the peak value of growth rate is $\gamma/\omega_c = 0.522046615$ appears at $\tilde{k} = 0.55$, for $A_T = 2$, growth rate is $\gamma/\omega_c = 0.59197259$ at $\tilde{k} = 0.55$ and as A_T is increasing to 2.25, peak value $\gamma/\omega_c = 0.656393317$ at $\tilde{k} = 0.5$. So, as we increase temperature anisotropy from 1.5 to 2.5, growth rate increases, and peaks appear to shift towards a lower value of wave number \tilde{k} .

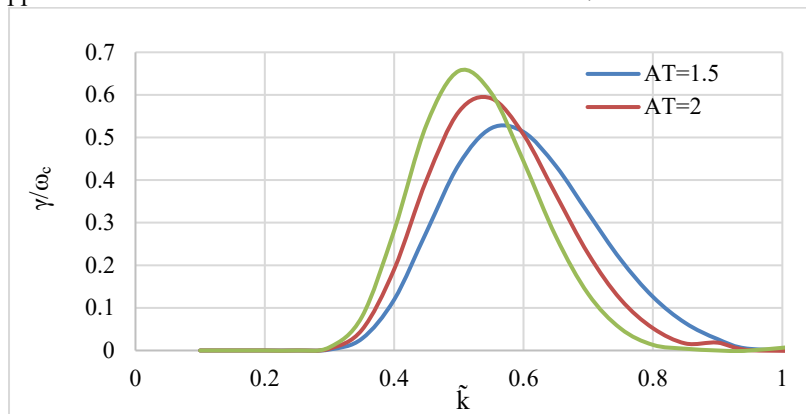


Figure 9. Variation of Growth Rate versus for different values of temperature anisotropy with beam with magnetic field model at $n_c/n_w = 1/10$, $\nu = 2$ Hz, $K_B T_{||i} = 1$ keV, $K_B T_{||ib} = 3$ keV, $K_B T_{||e} = 200$ eV, $B_0 = 5.1 \times 10^{-8}$ T, $E_0 = 0.1$ V/m and other fixed parameters of plasma at $17 R_J$

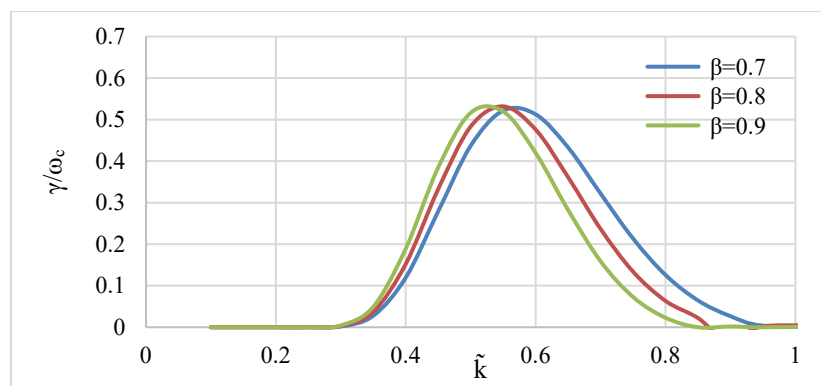


Figure 10. Variation of Growth Rate with relative to different values of relativistic factor with beam with magnetic field model at $n_c/n_w = 1/10$, $\nu = 2$ Hz, $A_T = 2$, $B_0 = 5.1 \times 10^{-8}$ T, $K_B T_{||i} = 1$ keV, $K_B T_{||ib} = 3$ keV, $K_B T_{||e} = 200$ eV, $E_0 = 0.1$ V/m and other fixed parameters of p

Figure 10 shows the effect of relativistic factor on growth rate with the effect of hot injected plasma with respect to \tilde{k} of electromagnetic ion-cyclotron waves using ring distribution function in the Jovian magnetosphere in the presence of external magnetic field model. It can be seen that for $\beta = 0.7$ the maxima occurs at $\tilde{k} = 0.5$ with $\gamma/\omega_c = 0.437003397$,

for $\beta=0.8$ the highest peak $\gamma/\omega_c = 0.48355298$ occurs at $\tilde{k}=0.5$ and for $\beta=0.9$ the peak value $\gamma/\omega_c = 0.516484702$ appears at $\tilde{k}=0.5$. It shows that growth increases for parallel propagation of EMIC wave in Jupiter's magnetosphere with increasing the magnitude of relativistic factor.

Figure 11 shows the effect of number density ratio of electrons and ions on growth rate after injecting hot plasma with respect to \tilde{k} of EMIC waves using ring distribution function at Jupiter. It can be observed that for $n_c/n_w = 1/10$ the maxima occurs at $\tilde{k} = 0.55$ with $\gamma/\omega_c = 0.522046615$, for $n_c/n_w = 1/20$ the highest peak $\gamma/\omega_c = 0.52839378$ occurs at $\tilde{k} = 0.55$ and for $n_c/n_w = 1/30$ the peak value $\gamma/\omega_c = 0.529800749$ appears at $\tilde{k} = 0.55$. It can be concluded that growth increases for parallel propagation of EMIC wave in Jupiter's magnetosphere as the magnitude increases. Thus, number density of electron does not affect the growth rate in the case of hot injection ion beam as [30] reported that dependence of dispersive properties of EMIC wave are on density and thermal plasma composition of ions.

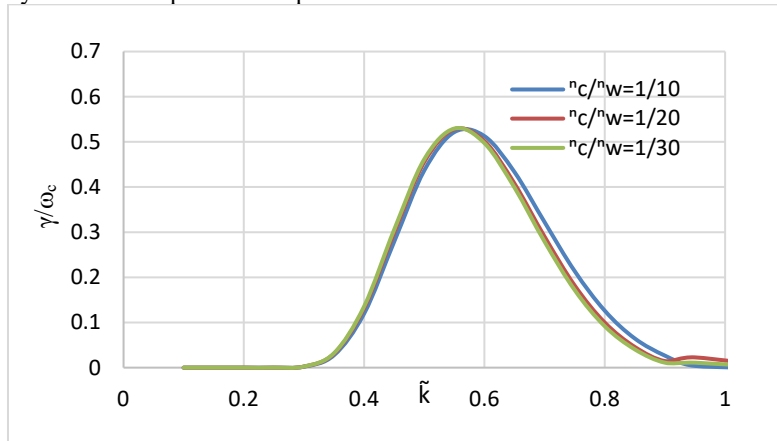


Figure 11. Variation of Growth Rate versus for different values of number density ratio (n_c/n_w) with beam with magnetic field model at $=2$ Hz, $A_T=2$, $K_{BT||i}=1$ keV, $K_{BT||ib}=3$ keV, $K_{BT||e}=200$ eV, $B_0=5.1 \times 10^{-8}$ T, $E_0=0.1$ V/m and other fixed parameters of plasma at 1

5. CONCLUSIONS

In this paper, parallel propagating electromagnetic ion-cyclotron waves have been investigated with the effect of hot injection for ring distribution in the presence of AC electric field in magnetosphere of Jupiter at a radial distance of $17 R_J$. To get better efficiency and consistency, kinetic approach has been performed. The detailed expression of dispersion relation, real frequency and growth rate has been derived for the parametric study. To analyze plasma parameters like AC frequency, temperature anisotropy etc., and graphs have been plotted with respect to wavenumber \tilde{k} . From the results, it is concluded that ion-cyclotron waves grows at Jupiter with increase in the values of temperature anisotropy, AC frequency and number density. After injecting hot ion beam, growth rate increases with the increasing AC frequency while it decreases as temperature anisotropy increases from 1.5 to 2.5. Graphs show that peak appears at the same value of wavenumber for an individual parameters.

Acknowledgement

We are thankful to our funding agency SERB and Dr. Ashok K. Chauhan (Founder President, Amity University), Dr. Atul Chauhan (President, Amity University) and Dr. Balvinder Shukla (Vice Chancellor, Amity University) for their immense encouragement.

ORCID

Garima Yadav, <https://orcid.org/0009-0005-3239-5996>; B.S. Sharma, <https://orcid.org/0000-0002-2327-9396>
Ankita, <https://orcid.org/0009-0009-2201-6453>

REFERENCES

- [1] J.M. Cornwall, *J. Geophys. Res.* **70**(1), 61 (1965). <https://doi.org/10.1029/JZ070i001p00061>
- [2] J.M. Cornwall, F.V. Coroniti, and R.M. Thorne, *J. Geophys. Res.* **75**(25), 4699 (1970)/ <https://doi.org/10.1029/JA075i025p04699>
- [3] B.J. Fraser, and T.S. Nguyen, *J. Atmos. Sol. Terr. Phys.* **63**(11), 1225 (2001). [https://doi.org/10.1016/S1364-6826\(00\)00225-X](https://doi.org/10.1016/S1364-6826(00)00225-X)
- [4] T.M. Loto'aniu, B.J. Fraser, and C.L. Waters, *J. Geophys. Res. Space Phys.* **110**(A7), (2005). <https://doi.org/10.1029/2004JA010816>
- [5] E. Kim, and J.R. Johnson, *Geophys. Res. Lett.* **43**(1), 13 (2016). <https://doi.org/10.1002/2015GL066978>
- [6] Z. Yuan, et al., "In situ evidence of the modification of the parallel propagation of EMIC waves by heated He + ions," *J. Geophys. Res. Space Phys.* **121**(7), 6711 (2016). <https://doi.org/10.1002/2016JA022573>
- [7] Y. Miyoshi, et al., *Geophys. Res. Lett.* **35**(23), (2008). <https://doi.org/10.1029/2008GL035727>
- [8] K. Hyun, K.-H. Kim, E. Lee, H.-J. Kwon, D.-H. Lee, and H. Jin, *J. Geophys. Res. Space Phys.* **119**(10), 8357 (2014). <https://doi.org/10.1002/2014JA020234>
- [9] Y. Omura, and D. Summers, *J. Geophys. Res. Space Phys.* **111**(A9), (2006). <https://doi.org/10.1029/2006JA011600>
- [10] S. Wu, H. Zhang, C. Zhou, S. Zhu, and X. He, *The European Physical Journal D*, **68**(7), 208 (2014). <https://doi.org/10.1140/epjd/e2014-50161-0>

- [11] R.C. Allen, *et al.*, J. Geophys. Res. Space Phys. **121**(7), 6458 (2016). <https://doi.org/10.1002/2016JA022541>
- [12] A.J. Halford, B.J. Fraser, and S.K. Morley, J. Geophys. Res. Space Phys. **115**(A12), (2010). <https://doi.org/10.1029/2010JA015716>
- [13] D. Wang, *et al.*, J. Geophys. Res. Space Phys. **120**(6), 4400 (2015). <https://doi.org/10.1002/2015JA021089>
- [14] R.E. Denton, V.K. Jordanova, and B.J. Fraser, J. Geophys. Res. Space Phys. **119**(10), 8372 (2014). <https://doi.org/10.1002/2014JA020384>
- [15] J.U. Kozyra, T.E. Cravens, A.F. Nagy, E.G. Fonthelm, and R.S.B. Ong, J. Geophys. Res. Space Phys. **89**(A4), 2217 (1984). <https://doi.org/10.1029/JA089iA04p02217>
- [16] R.M. Thorne, Geophys. Res. Lett. **37**(22), (2010). <https://doi.org/10.1029/2010GL044990>
- [17] E.H. Annex, R.S. Pandey, and M. Kumar, East Eur. J. Phys. (1), 40 (2022). <https://doi.org/10.26565/2312-4334-2022-1-06>
- [18] F. Bagenal, and P.A. Delamere, J. Geophys. Res. Space Phys. **116**(A5), (2011). <https://doi.org/10.1029/2010JA016294>
- [19] J. Kumari, and R.S. Pandey, Advances in Space Research, **63**(7), 2279 (2019). <https://doi.org/10.1016/j.asr.2018.12.013>
- [20] J. Kumari, R. Kaur, and R.S. Pandey, Astrophys. Space Sci. **363**(2), 33 (2018). <https://doi.org/10.1007/s10509-018-3250-0>
- [21] C. Cheverry, and A. Fontaine, J. Math. Anal. Appl. **466**(2), 1238 (2018). <https://doi.org/10.1016/j.jmaa.2018.06.045>
- [22] S. Kumar, S.K. Singh, and A.K. Gwal, Pramana, **68**(4), 611 (2007). <https://doi.org/10.1007/s12043-007-0063-z>
- [23] S. Agarwal, R.S. Pandey, and C. Jeyaseelan, Astrophys. Space Sci. **364**(8), 133 (2019). <https://doi.org/10.1007/s10509-019-3623-z>
- [24] M.G. Kivelson, and K.K. Khurana, J. Geophys. Res. Space Phys. **107**(A8), (2002). <https://doi.org/10.1029/2001JA000249>
- [25] B. Ni, *et al.*, Earth and Planetary Physics, **1**(2), 1 (2018). <https://doi.org/10.26464/epp2018001>
- [26] B.H. Mauk, D.J. Williams, and R.W. McEntire, Geophys. Res. Lett. **24**(23), 2949 (1997). <https://doi.org/10.1029/97GL03026>
- [27] J.T. Clarke, M.K. Hudson, and Y.L. Yung, J. Geophys. Res. Space Phys. **92**(A13), 15139 (1987). <https://doi.org/10.1029/JA092iA13p15139>
- [28] W.C. Feldman, J.R. Asbridge, S.J. Bame, and M.D. Montgomery, J. Geophys. Res. **78**(28), 6451 (1973). <https://doi.org/10.1029/JA078i028p06451>
- [29] D. Summers, and R.M. Thorne, J. Geophys. Res. Space Phys. **108**(A4), (2003). <https://doi.org/10.1029/2002JA009489>
- [30] A.A. Saikin, J.-C. Zhang, C.W. Smith, H.E. Spence, R.B. Torbert, and C.A. Kletzing, J. Geophys. Res. Space Phys. **121**(5), 4362 (2016). <https://doi.org/10.1002/2016JA022523>

ГЕНЕРАЦІЯ ЕЛЕКТРОМАГНІТНОЇ ІОННОЇ ЦИКЛОТРОННОЇ ХВИЛІ ШЛЯХОМ ГАРЯЧОЇ ІНЖЕКЦІЇ ІОННОГО ПУЧКА ДЛЯ КІЛЬЦЕВОГО РОЗПОДІЛУ З ЕЛЕКТРИЧНИМ ПОЛЕМ ЗМІННОГО ТОКУ В МАГНІТОСФЕРІ ЮПІТЕРА

Гаріма Ядав^a, Б.С. Шарма^a, Анкіта^b

^aФакультет фізики, Університет Лордса, Алвар-301001, Індія

^bДепартамент фізики, Інститут прикладних наук Аміті, Університет Аміті, Сектор-125 Нойда, Уттар-Прадеш, Індія

У цій статті досліджуються електромагнітні іонно-циклотронні хвилі, виявлені космічним кораблем «Улісс» у магнітосфері Юпітера. У цьому регіоні виявлено різні типи височастотного радіовипромінювання, що є результатом резонансної взаємодії. Дослідження зосереджено на взаємодії хвиля-частинка між електромагнітними іонно-циклотронними хвилями та повністю іонізованими частинками магнітосферної плазми, враховуючи паралельне поширення цих хвиль. Це дозволяє детально оцінити дисперсійне співвідношення з кільцевим розподілом за наявності паралельного електричного поля змінного струму (АС) у магнітосфері Юпітера без зіткнень. Використовуючи метод характеристик і кінетичний підхід, ми отримуємо вираз для релятивістської швидкості зростання. Крім того, ми аналізуємо події інжекції, зафіксовані космічним кораблем Galileo через його детектор енергетичних частинок (EPD) у магнітосфері Юпітера. Після введення гарячого іонного пучка ми проводимо параметричний аналіз різних параметрів плазми, таких як температурна анізотропія, частота змінного струму та релятивістські чинники, щоб дослідити їхній вплив на швидкість росту, що проілюстровано за допомогою нанесених графіків.

Ключові слова: електромагнітні іонно-циклотронні хвилі; кільцевий розподіл; ін'єкція гарячих іонів; магнітосфера Юпітера